J Mater Sci (2008) 43:3837–3847
DOI 10.1007/s10853-007-2220-7

Nanocrystallization of $Fe_{73.5}Si_{13.5}B_9Nb_3Cu_1$ soft-magnetic alloy from amorphous precursor in a magnetic field

Hiromichi Fujii · Victoria A. Yardley · Takashi Matsuzaki · Sadahiro Tsurekawa

Received: 7 July 2007 / Accepted: 10 October 2007 / Published online: 6 March 2008

Abstract The effect of a magnetic field on the nature of nanocrystallization from a melt-spun $Fe_{73.5}Si_{13.5}B_9Nb_3Cu_1$ amorphous precursor has been studied with the aim of controlling microstructures and magnetic properties. Annealing for magnetic crystallization was carried out at temperatures between the Curie temperature of the amorphous phase (586 K) and that of the crystalline phase (920 K). It was found that the {110} texture component in crystallized α-Fe(Si) phase increased in importance with increasing magnetic-field strength. An X-ray diffraction analysis based on the Shultz method revealed that the magnetic field caused preferential formation of {110}-oriented nuclei. In addition, the applied field enhanced crystallization kinetics, particularly the nucleation rate. No significant difference in grain growth behavior was observed as a result of applying a magnetic field. We therefore conclude that the development of the {110} texture by magnetic crystallization is predominantly attributable to preferential nucleation, rather than preferential growth, of {110}-oriented nuclei. The saturation magnetization of nanocrystallized specimens, evaluated using a vibrating sample magnetometer (VSM), was increased by the application of a magnetic field up to 4T during nanocrystallization.

H. Fujii (✉) · V. A. Yardley · T. Matsuzaki
Department of Nanomechanics, Graduate School of Engineering, Tohoku University, Sendai 980-8579, Japan
e-mail: fujii@md.mech.tohoku.ac.jp

S. Tsurekawa
Faculty of Engineering, Kumamoto University, Kumamoto 860-8555, Japan

Introduction

Soft-magnetic materials are widely used in modern technological applications such as transformers, hard disk drives, and mobile phones. Nanocrystalline (nc) iron-based materials like FINEMET [1, 2] have been found to show superior magnetic softness than in their purely amorphous phase. There are several processing routes for production of nc-materials [3]. Crystallization from an amorphous precursor is one of the most important of these, and therefore extensive studies on this processing route have been conducted [3] since Yoshizawa et al. found that nc-Fe–Si–B–Nb–Cu alloy produced by crystallization from an amorphous precursor possessed excellent soft-magnetic properties [1]. It is well known that the degree of magnetic softness is significantly influenced by microstructure [4, 5]. Most previous studies concentrate primarily on the control of the size and morphology of crystallites. However, in addition to this, crystal orientation and its distribution (texture) are important microstructural factors controlling magnetic softness. Therefore, if we can control the microstructure of iron-based nc-materials more precisely, further enhancement of soft-magnetic properties should be possible.

In this work, we have considered the application of a magnetic field during nanocrystallization by annealing from an iron-based amorphous precursor. Because crystallization from an amorphous phase involves much less restriction from existing microstructure than a crystalline-to-crystalline phase transformation such as recrystallization and grain growth, a more significant field-induced effect on the development of the microstructure can be expected. In our previous study, we found that the magnetic crystallization ($H = 6$ T) of an $Fe_{78}Si_9B_{13}$ amorphous precursor at 853 K, which is between the Curie temperature of the amorphous phase and that of the α-Fe(Si) crystalline phase,

causes the development of a sharp {110} texture in the microcrystalline alloy [6]. In earlier work on magnetic crystallization from amorphous precursors, Häußler and Baumann [7] reported first in 1980 that the crystallization temperatures of amorphous Bi, Ga, and Yb were not affected by a magnetic field of 18.5 T. However, Wolfus et al. [8] investigated the effect of a magnetic field (ranging from 3 mT to 1 T) on the crystallization kinetics of $Fe_{83}Si_5B_{12}$ amorphous alloy, and found that the crystallization of ferromagnetic phase increased with increasing field. Otani et al. [9] studied magnetic crystallization of a melt-spun $Pr_2Co_{14}B$ amorphous alloy for the purpose of controlling grain orientation. They found that crystallization in a 0.3 T magnetic field slightly enhanced the development of a texture, with the easy magnetization *c*-plane oriented along the magnetic field direction. Recently, Wang et al. [10] have investigated the effect of a magnetic field on the nucleation of crystallites of diamagnetic tI-Zr_2Cu, fcc-Zr_2Ni, and hp-Zr_6Al_2Ni phases in $Zr_{62}A_{l8}Ni_{13}Cu_{17}$ amorphous alloys. They mentioned that the difference between the permeability of the amorphous phase and that of the crystalline phase suppressed crystallization in a magnetic field.

From these results, one can understand that a new strategy of magnetic crystallization can be a useful tool for controlling microstructure and crystallization kinetics. However, to the authors' knowledge, this strategy has not yet been applied to nanocrystallization. It is also of great interest to know how magnetic properties of nc-materials change according to magnetic crystallization. The aim of the present work is thus to investigate the effect of a magnetic field on the nanocrystallization of the $Fe_{73.5}Si_{13.5}B_9Nb_3Cu_1$ amorphous alloy with particular emphasis on texture formation, nanocrystallization kinetics, and the magnetic properties resulting from magnetic crystallization.

Experimental

Magnetic crystallization

An $Fe_{73.5}Si_{13.5}B_9Nb_3Cu_1$ melt-spun amorphous ribbon of 15 mm in width and 18 μm in thickness, which was supplied by Hitachi Metals Ltd., was used as the starting material in this study. A differential scanning calorimeter (DSC, Netzsch DSC-404C) was used to determine the Curie temperature of the amorphous (T_c^{Am}) and that of the crystalline phase (T_c^X) and the crystallization temperature (T_x). The DSC measurements were carried out at a heating rate of 0.33 K/s (20 K/min) in an Ar gas flow of 50 mL/s. The measured specific temperatures are shown in Table 1. The annealing conditions for magnetic crystallization, which were determined on the basis of the specific temperatures, are exhibited in Table 2. The annealing temperatures, ranging from 723 K to 823 K, were chosen to be between the Curie temperature of the amorphous phase and that of the crystalline phase, which allows ferromagnetic crystallites to be formed in a paramagnetic amorphous phase. The specimens to be crystallized were cut from the amorphous ribbon with dimensions of 10 mm × 5 mm, and then sandwiched by tungsten sheets to prevent contamination from the carbon holder used for annealing. The annealing treatments were carried out in a vacuum of 1.0×10^{-3} Pa under magnetic fields of up to 6 T using a superconducting magnetic-field heat treatment system composed of a helium-free superconducting magnet (Sumitomo Heavy Machine Corporation) and a high-temperature furnace with a molybdenum sheet heating element (Futek Furnace Inc.). The magnetic field was applied parallel or perpendicular to the surface of the specimen.

Table 1 Measured specific temperatures in $Fe_{73.5}Si_{13.5}B_9Nb_3Cu_1$ alloy

Material	Curie temperature of amorphous phase, T_c^{AM} (K)	Crystallization temperature, T_x (K)	Curie temperature of crystalline phase, T_c^X (K)
$Fe_{73.5}Si_{13.5}B_9Nb_3Cu_1$	586	750	920

Table 2 Annealing conditions for magnetic crystallization of $Fe_{73.5}Si_{13.5}B_9Nb_3Cu_1$ amorphous alloy

Material	Temperature, T (K)	Time, t (ks)	Magnetic field	
			Strength, H (T)	Direction
$Fe_{73.5}Si_{13.5}B_9Nb_3Cu_1$	723	1.4	0, 2, 4, 6	H // surface, $H \perp$ surface
	723	2.6	0, 2, 4, 6	
	723	4.4	0, 2, 4, 6	
	773	2.6	0, 2, 4, 6	
	793	2.6	0, 2, 4, 6	
	823	2.6	0, 2, 4, 6	

Observations of microstructure and measurements of magnetic properties

An X-ray diffractometer (XRD, RIGAKU JDX-3530) was used to observe the progress of crystallization and to identify the crystalline phases. In addition, the texture of the assembly of grains after crystallization was evaluated using the orientation index $R(hkl)$ given by the following equation [11],

$$R(hkl) = \frac{I(hkl)}{\Sigma I(h'k'l')} \Big/ \frac{I_0(hkl)}{\Sigma I_0(h'k'l')}, \quad (1)$$

where $I(hkl)$ is the XRD intensity obtained from experimental data and $I_0(hkl)$ is the intensity from a standard powder diffraction measurement. The orientation distribution of nuclei was analyzed by the X-ray Shultz method using specimens at an early stage of crystallization, where individual nucleated crystals had not yet met each other; this condition was obtained by annealing at 723 K for 1.8 ks without and with a 6 T magnetic field.

In order to examine the effect of a magnetic field on the kinetics of nucleation and growth in the amorphous alloy, transmission electron microscopy (TEM) was applied to observe microstructural change in the specimens annealed at 723, 773, and 793 K for 1.4, 2.6, and 4.4 ks without and with 6 T magnetic fields. Thin foils suitable for TEM observation were prepared by atom-milling at 5 kV and 2 mA with a beam angle of 15°, using an apparatus equipped with a cooling stage using liquid nitrogen. Conventional TEM observations were performed on a HITACHI HF-2000 FEG-TEM operated at an accelerating voltage of 200 kV. From the TEM micrographs, the number density of nuclei per unit volume, the grain size distribution, and the volume fraction of crystallized phase were statistically analyzed. To determine the volume of the observed area, the thickness of the area of interest was measured using a contamination-spot separation method [12].

The magnetic properties of the crystallized specimens were measured at room temperature using a vibrating sample magnetometer (VSM) from Tamakawa Co. Ltd., and discussed in terms of the observed microstructures.

Results and discussion

Microstructure evolution in a magnetic field

Figure 1 shows TEM micrographs of $Fe_{73.5}Si_{13.5}B_9Nb_3Cu_1$ specimens crystallized at 823 K for 2.6 ks (a) without and (b) with a 6 T magnetic field applied parallel to the ribbon surface. Selected area electron diffraction (SAD) patterns obtained from the same area as the TEM micrographs are also shown in Fig. 1. Both specimens are composed of a residual amorphous phase and a nanocrystalline phase. There appears to be no significant difference between the microstructure of the two specimens. The average grain size of the crystalline phase, which is determined to be α-Fe(Si), as shown in Fig. 2, is approximately 15–20 nm irrespective of whether a magnetic field is applied.

X-ray diffraction profiles for the specimens crystallized by annealing at 823 K for 2.6 ks with different field strengths are shown in Fig. 2. For comparison, the profile for the as-spun specimen is shown in the figure as well. Only some peaks associated with α-Fe(Si) phase are observed. No other phases except α-Fe(Si) were recognized from the XRD profiles. Of particular importance is the finding that the intensity of the {110} peak increases with increasing magnetic-field strength. The degree of texture was evaluated by means of the orientation index defined in Eq. 1 from the XRD profiles, and the variation of this value with field strength is shown in Fig. 3. The orientation index for the {110} reflection is a monotonically increasing function of magnetic-field strength, indicating an increase of sharpness of the {110} texture as a result of magnetic crystallization. Here a question arises as to whether the {110} texture is induced by preferential nucleation or by preferential growth. In order to examine further the influence of a magnetic field on the orientation of nuclei, X-ray diffraction based on the Shultz method was applied to the

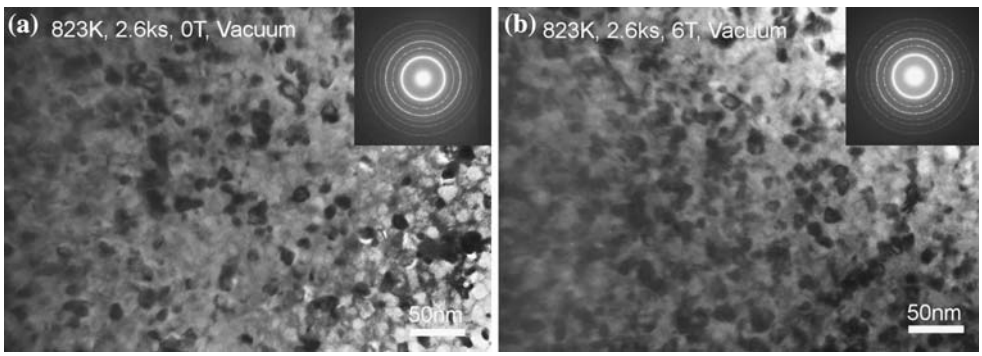

Fig. 1 Bright-field TEM micrographs and diffraction patterns for the $Fe_{73.5}Si_{13.5}B_9Nb_3Cu_1$ ribbons nanocrystallized from an amorphous precursor by annealing at 823 K for 2.6 ks (**a**) without and (**b**) with a 6 T magnetic field

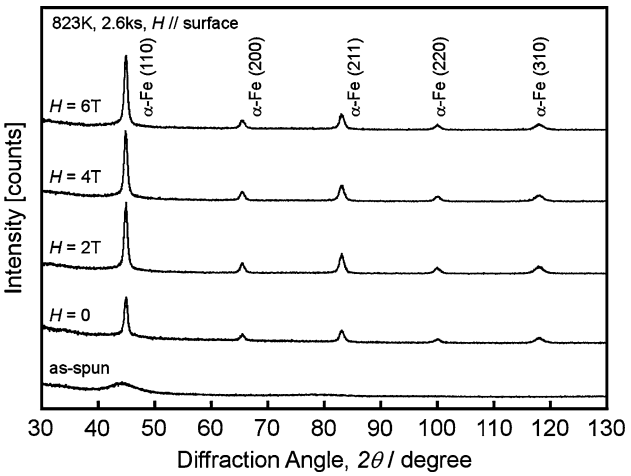

Fig. 2 X-ray diffraction profiles for the $Fe_{73.5}Si_{13.5}B_9Nb_3Cu_1$ ribbons crystallized at 823 K for 2.6 ks with different magnetic-field strengths. The magnetic field was applied parallel to the ribbon surface

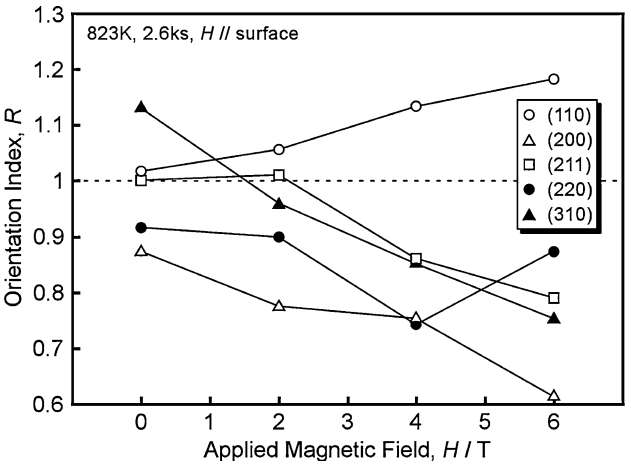

Fig. 3 Orientation index for (*hkl*) reflections for $Fe_{73.5}Si_{13.5}B_9Nb_3Cu_1$ ribbons crystallized at 823 K for 2.6 ks as a function of magnetic-field strength

specimen at an early stage of crystallization from the amorphous phase, where the individual nucleated grains had not yet met each other. Figure 4 shows 110 pole figures from specimens annealed at 723 K for 2.6 ks without and with a 6 T magnetic field. The {110} poles of the assembly of crystallites are found to be somewhat localized at the center of the pole figure in the specimen crystallized with a 6 T magnetic field compared with those in the specimen annealed without a magnetic field; the intensity of {110} poles at the center is higher by about 25% in the magnetically annealed case. One may expect that one of the ⟨001⟩ directions which are the easy magnetization directions in bcc-iron, might be aligned along the magnetic field direction in α-Fe(Si) crystals. However, there is no significant evidence of localization of {110} poles anywhere except at the center of the pole figure even in the specimen crystallized with a 6 T magnetic field. From these results, we can conclude that the {110}-oriented nuclei are formed preferentially in a magnetic field, and one of the ⟨001⟩ orientations in these nuclei is oriented in a random direction in the plane of the ribbon surface. This result is in good agreement with previous work on magnetic crystallization from an $Fe_{78}Si_9B_{13}$ amorphous alloy.

Regarding grain growth in a magnetic field, grain size distributions were examined in specimens crystallized under various annealing conditions. Figure 5 presents changes in the grain size distribution with annealing time for specimens crystallized at 723 K without and with a 6 T magnetic field. These closely resemble normal distributions whether or not a magnetic field is applied; this indicates that normal grain growth of α-Fe(Si) crystals occurs both with and without magnetic field. Looking through Fig. 5a–f, we can see that the average grain size and the standard deviation both change only very slightly with annealing time, and there is no observable difference between the nature of grain growth without and with a 6 T magnetic field. A similar result is observed at different temperatures as shown in Fig. 6. Unlike the magnetic crystallization of the $Fe_{78}Si_9B_{13}$ alloy, in which energetically preferred {110} grains grew faster and a bimodal grain size distribution developed in a magnetic field [6], grain growth in the $Fe_{73.5}Si_{13.5}B_9Nb_3Cu_1$ alloy does not appear to be affected by a magnetic field. This lack of influence on grain growth by the magnetic field is probably attributable to the mechanisms believed to be responsible for the extremely slow grain growth in this alloy under ordinary annealing conditions. These are either that Cu clusters formed in the amorphous phase prevent the migration of the interface between the crystallite and the amorphous phase, or that the diffusivity of Nb atoms that are rejected from α-Fe(Si) crystallites to the amorphous phase is very low [13]. The increased driving force for grain growth of preferred orientations under a magnetic field may be insufficient compared to the forces, mentioned above, that resist grain growth. Judging from Figs. 2 to 5, we can conclude that preferential nucleation of {110}-oriented grains, rather than preferential growth, is the predominant reason for the development of {110} texture in the nc-$Fe_{73.5}Si_{13.5}B_9Nb_3Cu_1$ alloy annealed under a magnetic field.

Another question arises, of why the {110} orientation is preferentially nucleated in a magnetic field. In the previous report on the magnetic crystallization of the $Fe_{78}Si_9B_{13}$ alloy, we discussed the reason for the {110} texture formation from the point of view of magnetocrystalline anisotropy energy on the basis of observations suggesting preferential growth of {110}-oriented α-Fe(Si) grains [6]. However, since no significant effect of a magnetic field was observed on the grain growth in the

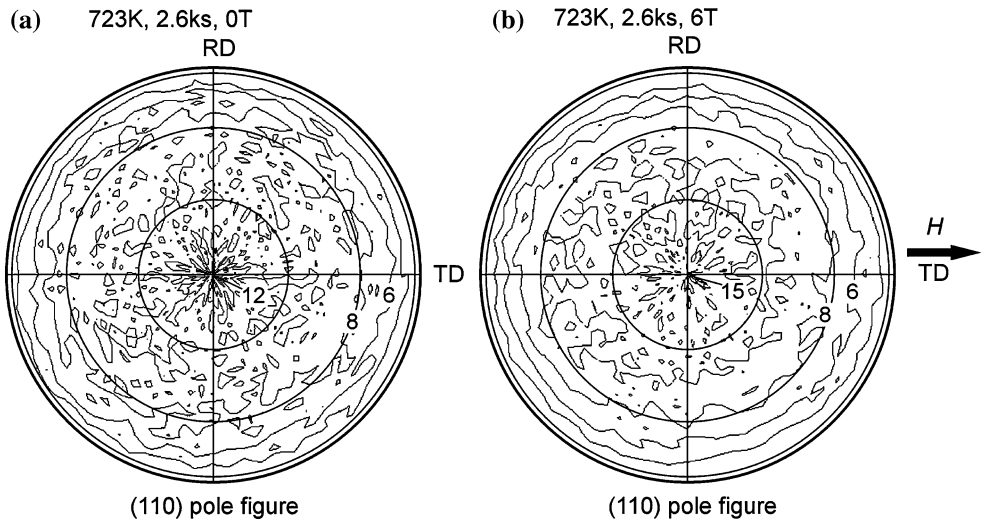

Fig. 4 {110} pole figures for $Fe_{73.5}Si_{13.5}B_9Nb_3Cu_1$ ribbons after annealing at 723 K for 2.6 ks (**a**) without and (**b**) with a 6 T magnetic field parallel to the ribbon surface

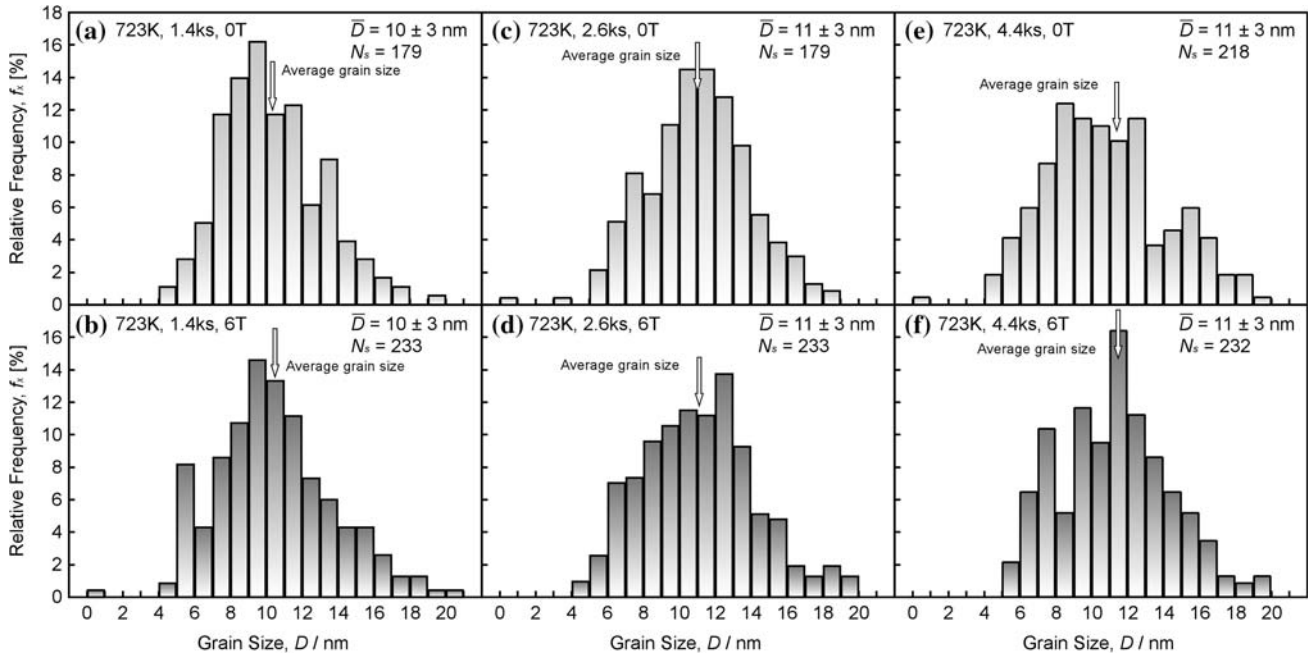

Fig. 5 Changes in the grain size distribution in the nc-$Fe_{73.5}Si_{13.5}B_9Nb_3Cu_1$ alloy with annealing time at 723 K without (**a**, **c**, **e**) and with (**b**, **d**, **f**) a 6 T magnetic field

nc-$Fe_{73.5}Si_{13.5}B_9Nb_3Cu_1$ alloy, a similar explanation based on the anisotropy energy seems to be insufficient to explain the preferential nucleation of {110} oriented grains observed. Several possible reasons for this should be further considered: e.g., the influence of a magnetic field on surface energy.

Volume fraction of nanocrystallized grains in a magnetic field

In our previous study on magnetic crystallization of the $Fe_{78}Si_9B_{13}$ alloy, it was found that the volume fraction of the crystalline α-Fe(Si) phase was increased by application of a 6 T magnetic field [6]. Accordingly, we evaluated the volume fraction of the nanocrystalline α-Fe(Si) phase in the $Fe_{73.5}Si_{13.5}B_9Nb_3Cu_1$ alloy using an XRD profile fitting procedure [14, 15]. The XRD {110} peak was fitted according to the pseudo-Voigt function given by the following equation,

$$V(x) = (1 - \eta)L(x) + \eta G(x), \tag{2}$$

where $L(x)$ and $G(x)$ are the Lorentzian and Gaussian functions, respectively, and η represents the Gaussian contribution to the peak. (Here it was assumed that the

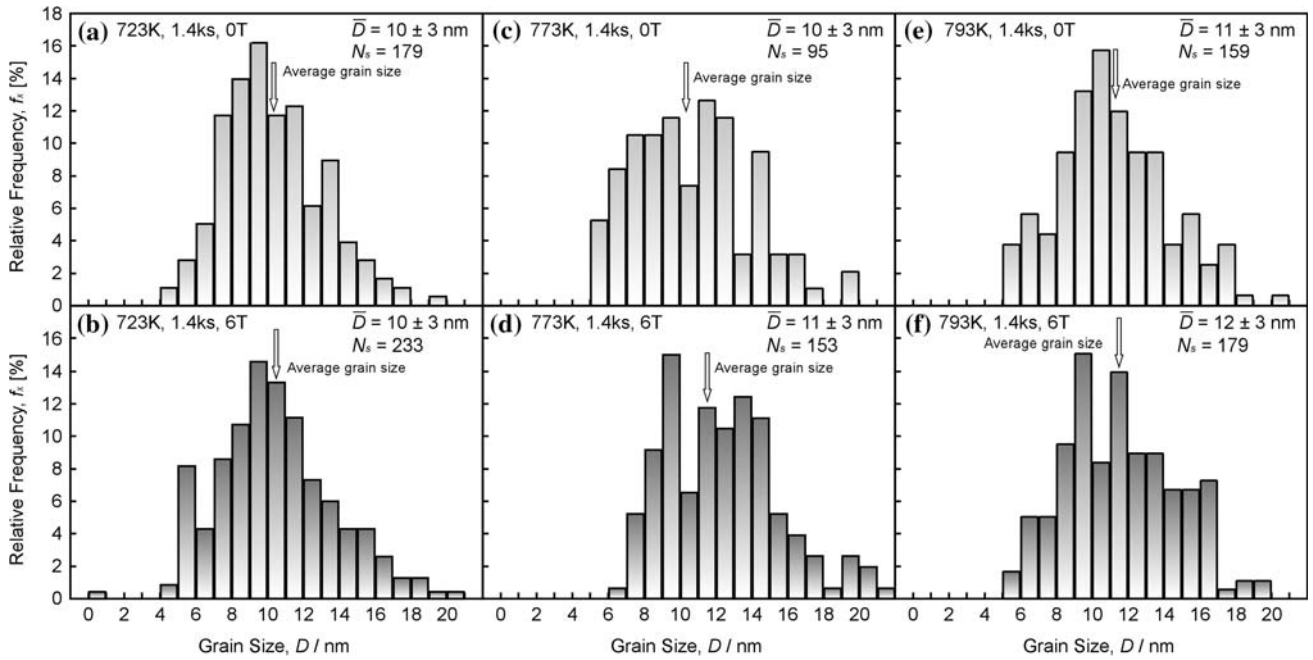

Fig. 6 Changes in the grain size distribution in the nc-$Fe_{73.5}Si_{13.5}B_9Nb_3Cu_1$ alloy with annealing temperature for an annealing time of 1.4 ks without (**a**, **c**, **e**) and with (**b**, **d**, **f**) a 6 T magnetic field

XRD profiles from the amorphous and crystalline phases could be expressed by Lorentzian and Gaussian functions, respectively.) Figure 7 exhibits the volume fraction of α-Fe(Si) phase crystallized from the $Fe_{73.5}Si_{13.5}B_9Nb_3Cu_1$ amorphous precursor by annealing at 823 K for 60 s to 1.8 ks as a function of magnetic-field strength. Considering the data for each value of magnetic field strength, there is no systematic variation of volume fraction with annealing time. Taking account of experimental error, it is considered that the fraction crystallized may have almost approached saturation even after annealing for only 60 s at 823 K.

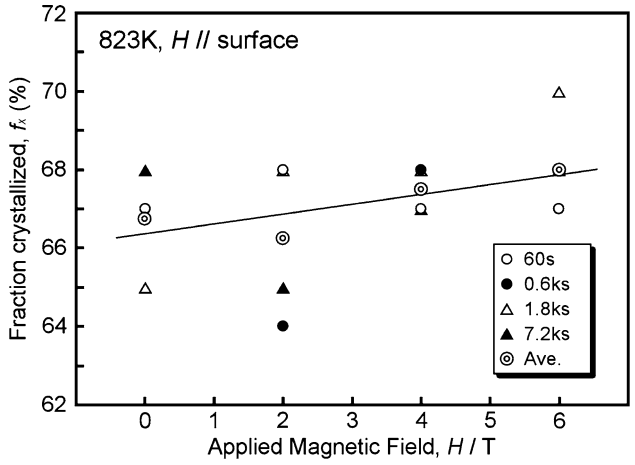

Fig. 7 Volume fraction of α-Fe(Si) phase crystallized from $Fe_{73.5}Si_{13.5}B_9Nb_3Cu_1$ amorphous precursor by annealing at 823 K for 60 s to 1.8 ks as a function of a magnetic-field strength

However, by observing the average values, the volume fraction of α-Fe(Si) phase somewhat increases with increasing magnetic-field strength, from 67% at zero field to 68% at 6 T magnetic field. These estimated values of volume fraction crystallized are in good agreement with those previously reported for nc-$Fe_{73.5}Si_{13.5}B_9Nb_3Cu_1$ alloy produced by fully annealing at similar temperatures [14–17]. Regarding the increase in the volume fraction of α-Fe(Si) phase by magnetic crystallization, we have discussed the possibility of change in the equilibrium phase stability due to the energetic contribution of the magnetic field [18]. However, one of the present authors (V.Y.) has recently calculated the contribution of the magnetic free energy to the total Gibbs free energy on the basis of CALPHAD methodology [19], and pointed out that the energetic contribution from an applied magnetic field of 6 T was insufficient to predict the changes in α-Fe phase fraction in nc-$Fe_{73.5}Si_{13.5}B_9Nb_3Cu_1$ reported here, or the larger phase fraction differences observed in $Fe_{78}Si_9B_{13}$ [6]. To obtain the changes in the α-Fe fraction observed experimentally, a magnetic energy contribution of the order of -2 kJ mol^{-1} would be needed. This energy corresponds to an applied field of 180 T. A possible explanation for the observed differences in phase fraction (discussed in more detail in [19]) is that the magnetic energy contribution, by increasing the nucleation rate, results in nuclei of crystalline phase in an amorphous matrix that still contains some quenched-in excess energy from the melt-spinning process. Slower nucleation kinetics,

by contrast, would allow the matrix time to relax and to lower its energy. The position of local equilibrium between the amorphous and crystalline phases, and therefore the fraction of crystalline phase formed, would thus be different in the two cases. However, this explanation is still speculative and further investigation is needed in this area.

Crystallization kinetics in a magnetic field

In order to study the effect of a magnetic field on the kinetics of nucleation and growth in the $Fe_{73.5}Si_{13.5}B_9Nb_3Cu_1$ amorphous alloy, TEM was used to observe the progress in crystallization, particularly at the early stages. Figure 8 shows TEM micrographs of specimens crystallized at 723 K for 1.4 ks (a) without and (b) with a 6 T magnetic field. The SAD patterns from each specimen are also exhibited in the figures. From these micrographs, the number of crystallites appears to be higher in the specimen annealed with a 6 T magnetic field than without a magnetic field. In addition, the SAD pattern from the specimen annealed without a magnetic field displays a broader ring shape, whereas the ring pattern from the specimen annealed with a 6 T magnetic field is clearer and sharper. Consequently, it is considered that a magnetic field can enhance the nucleation rate of ferromagnetic α-Fe(Si) grains from the paramagnetic amorphous phase.

We quantitatively evaluated the number density of nuclei per unit volume as a function of annealing time as shown in Fig. 9a. The number density appears to be an exponential function of annealing time irrespective of whether or not a magnetic field is applied. However, values were increased by 2–3 times by the application of a 6 T magnetic field. Anderson and Mehl found that the nucleation rate $\dot{N}_n$ as a function of annealing time in the recrystallization of aluminum was given by the following exponential function, at least up to 30% recrystallization [20].

$$\dot{N}_n = a\exp(bt), \tag{3}$$

where a and b are constants. Figure 9b shows the semi-logarithm plots of the number density of nuclei against annealing time. There is a good linear correlation between the natural logarithms of N_n and annealing time for specimens crystallized both without and with a magnetic field. Therefore, Eq. 3 can be applied for magnetic crystallization of the nc-$Fe_{73.5}Si_{13.5}B_9Nb_3Cu_1$ alloy. The values of a and b in Eq. 3 were estimated to be $a = 1.2 \times 10^{21}\ m^{-3}\ s^{-1}$, $b = 0.23$ for crystallization with a 6 T magnetic field and $a = 5.2 \times 10^{20}\ m^{-3}\ s^{-1}$, $b = 0.20$ without a magnetic field.

Changes in the volume fraction of the α-Fe(Si) crystalline phase f_x during crystallization of the $Fe_{73.5}Si_{13.5}B_9Nb_3Cu_1$ amorphous precursor by annealing at 723 K without and with a 6 T magnetic field are shown in Fig. 10a and b. To determine the volume of each grain, grains were assumed to have a spherical shape. The volume fraction is found to be increased by 2–3 times by the application of a magnetic field, as shown in Fig. 10a. The dependence of the crystallized fraction on annealing time was examined on the basis of the Johnson–Mehl–Avrami–Kolmogorov (JMAK) equation given by

$$f_x = 1 - \exp(-Kt^n), \tag{4}$$

$$K = f\,\dot{N}_n\dot{G}^3, \tag{5}$$

where f is a shape factor ($4\pi/3$ for spheres) and $\dot{G}$ the growth rate. From the JMAK plot of the crystallization kinetics of the $Fe_{73.5}Si_{13.5}B_9Nb_3Cu_1$ alloy shown in Fig. 10b, the Avrami indices of the specimens crystallized without and with a 6 T magnetic field were estimated to be 0.65 and 0.74, respectively. The value of K, which is a function of both the nucleation rate and the growth rate of the grains, was higher by 2.2 times with the 6 T magnetic field (4.47×10^{-3}) than without the magnetic field (2.02×10^{-3}). As mentioned above, the nucleation rate was increased by 2–3 times by the application of a magnetic field, but the growth rate was not significantly affected by a magnetic field. Therefore, it is considered that the increase in the volume fraction of crystallized phase

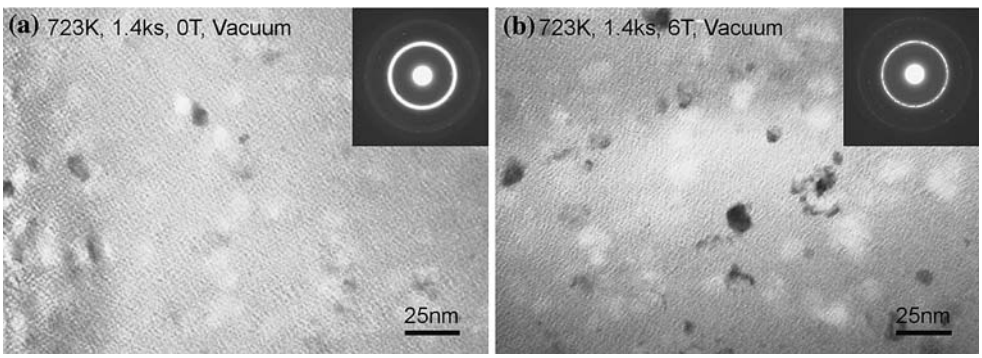

Fig. 8 Bright-field TEM micrographs and diffraction patterns for $Fe_{73.5}Si_{13.5}B_9Nb_3Cu_1$ ribbons at an early stage of crystallization obtained by annealing at 723 K for 1.4 ks (**a**) without and (**b**) with a 6 T magnetic field

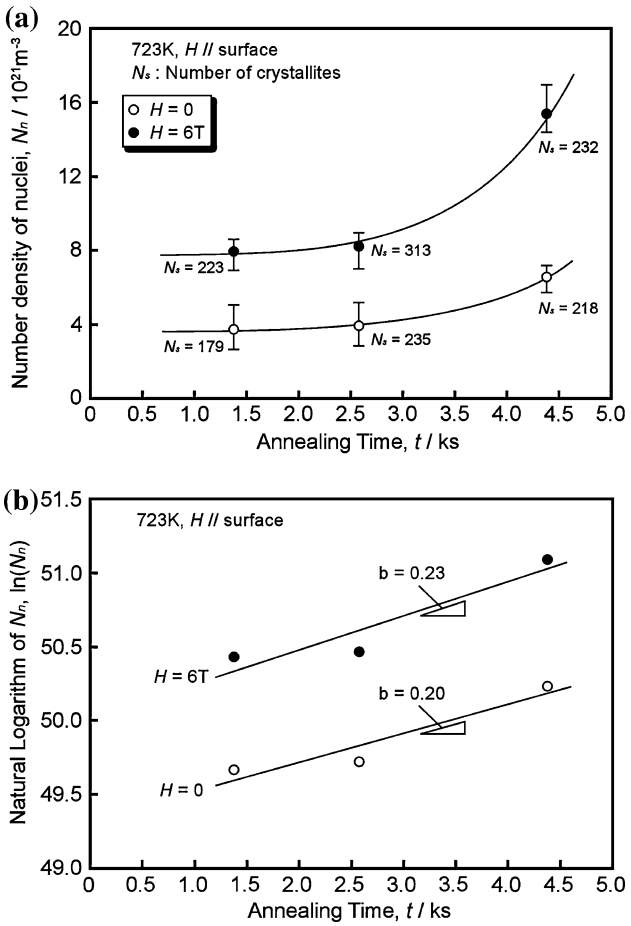

Fig. 9 Changes in number density of nuclei per unit volume in the $Fe_{73.5}Si_{13.5}B_9Nb_3Cu_1$ amorphous precursor with annealing time at 723 K without and with a 6 T magnetic field: (**a**) normal plot and (**b**) semi-logarithm plot of number density against annealing time

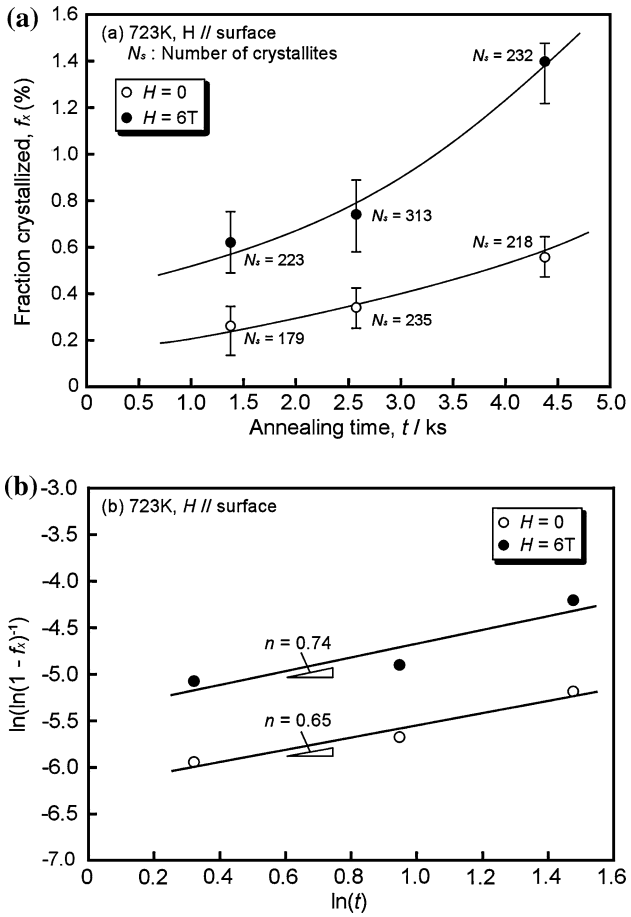

Fig. 10 Changes in volume fraction of α-Fe(Si) phase crystallized from $Fe_{73.5}Si_{13.5}B_9Nb_3Cu_1$ amorphous precursor with annealing time at 723 K without and with a 6 T magnetic field: (**a**) normal plot and (**b**) JMAK plot of fraction crystallized against annealing time

due to a magnetic field is predominantly caused by the increase in nucleation rate rather than by any change in the growth rate.

Origin of the enhancement of crystallization kinetics in a magnetic field

According to the classical nucleation-growth theory, the activation energy barrier against nucleation, ΔG^*, is determined from the free-energy change per unit volume, ΔG_V, associated with the phase transformation, and the interface energy, γ, between the nucleus and the amorphous matrix. In addition, a magnetic contribution to the volume free energy should be considered in a magnetic field because the ferromagnetic α-Fe(Si) phase is formed from the paramagnetic amorphous phase. Therefore, the activation energy for nucleation, ΔG^*, and the critical radius for nucleation r^*, in a magnetic field are given by the following equations:

$$\Delta G^* = \frac{16\pi\gamma^3}{3(\Delta G_v + \Delta G_M)^2}, \tag{6}$$

$$r^* = -\frac{2\gamma}{\Delta G_v + \Delta G_M}, \tag{7}$$

where ΔG_M is the change in magnetic free energy associated with crystallization. Ignoring any influences of the magnetic field on the interface energy, and assuming that the magnetic free energy of the paramagnetic amorphous phase is negligible, the values of ΔG^* and r^* will decrease in a magnetic field as shown in Fig. 11a because both ΔG_V and ΔG_M are negative. Thus, the nucleation of the ferromagnetic α-Fe(Si) phase will be made easier by application of a magnetic field.

Here, let us look at Fig. 9 again. When the exponential curves showing the relation between the number density of nuclei N_n and the annealing time t are interpolated to $t = 0$, the curves intersect the vertical axis at a finite value irrespective of whether a magnetic field is applied; the number

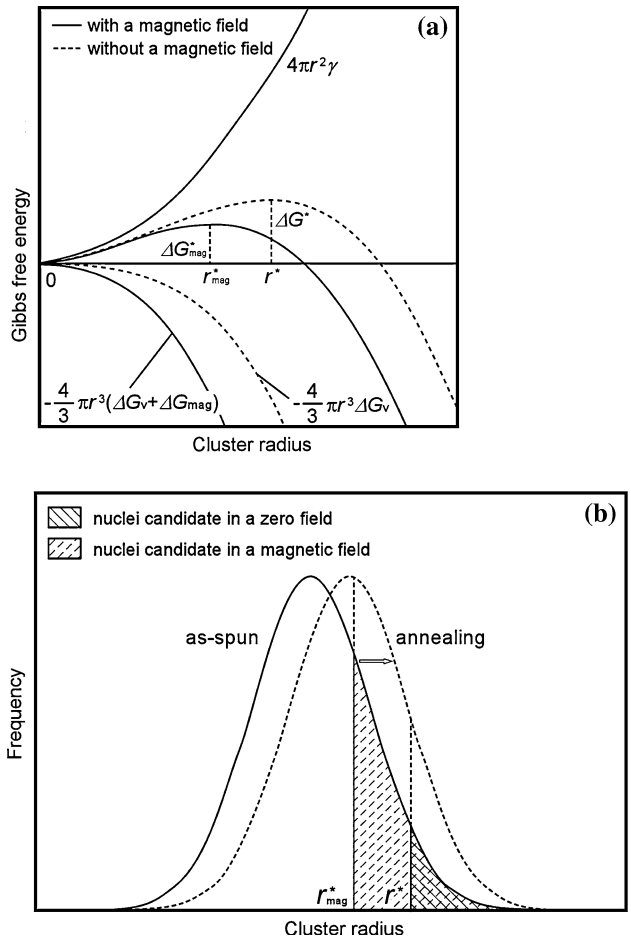

Fig. 11 Schematic explanation of (**a**) the influence of a magnetic field on the activation energy of nucleation and the critical nucleus size, and (**b**) a possible reason for the increase in nucleation rate under a magnetic field

density of nuclei does not become zero at $t = 0$. This is probably because some short-range ordered clusters (embryos), which could subsequently become the cores of nucleating crystals, may have existed in the amorphous precursor, unlike in the case of nucleation of crystals from a liquid phase. If we assume that the size distribution of the clusters is Gaussian, the number of clusters (embryos) that are super-critical and can grow into stable grains would increase with a decrease in the critical radius due to a magnetic field, as illustrated in Fig. 11b. Furthermore, if the size distribution of clusters could shift to a regime of larger cluster size by annealing, an increase in the nucleation rate would be higher in a magnetic field than in zero-field.

An attempt is made to test this proposition using some data from literature and from equilibrium calculations in the framework of the CALPHAD methodology. The magnetic free energy per unit volume for ferromagnetic materials is given by

$$\Delta G_{\mathrm{M}}^{\mathrm{f}} = -\mu_0\left(H - \frac{NM_{\mathrm{s}}}{2}\right)M_{\mathrm{s}} \tag{8}$$

where μ_0 is the permeability in vacuum, N is the demagnetizing factor, and M_{s} is the saturation magnetization. In our experiments, a magnetic field was applied parallel to the long axis of the ribbon, so that the demagnetizing factor is assumed to be zero. The saturation magnetization of the crystalline phase was estimated to be $\mu_0 M_{\mathrm{s}} = 1.82$ T (=kg/s^2 A) for the composition of $Fe_{73.5}Si_{13.5}$ by assuming that it decreases with increasing Si content according to the data for the magnetic moment of Fe–Si alloys as a function of Si content found in [21]. From Eq. 8, we can obtain a value of the magnetic free energy, $\Delta G_{\mathrm{M}}^{\mathrm{f}} = 8.69 \times 10^6$ J/m^3 in a 6 T magnetic field. The value of ΔG_{v} was calculated using the CALPHAD methodology for a nucleus of equilibrium composition ($Fe_{77}Si_{18}Nb_4Cu_1$), forming at 823 K in a matrix of composition $Fe_{73.5}Si_{13.5}B_9Nb_3Cu_1$ and a value of approximately 8.0×10^8 J/m^3 obtained. A surface energy of $\gamma = 1.850$ J/m^2, which was reported for a Fe-3 wt%Si alloy [22, 23], was used. Consequently, the critical radius of a nucleus in zero-field and that in a 6 T magnetic field are estimated to be 4.63 nm and 4.57 nm, respectively. The difference between these values seems to be insufficient to predict the large changes in nucleation rate observed experimentally.

Magnetic properties of nc-$Fe_{73.5}Si_{13.5}B_9Nb_3Cu_1$ alloy crystallized in a magnetic field

Magnetic properties of the nc-$Fe_{73.5}Si_{13.5}B_9Nb_3Cu_1$ alloy crystallized at 823 K for 2.6 ks in a magnetic field are shown in Fig. 12. For comparison, a magnetization curve for the amorphous precursor is also shown. The saturation magnetization of the nanocrystallized specimen is found to

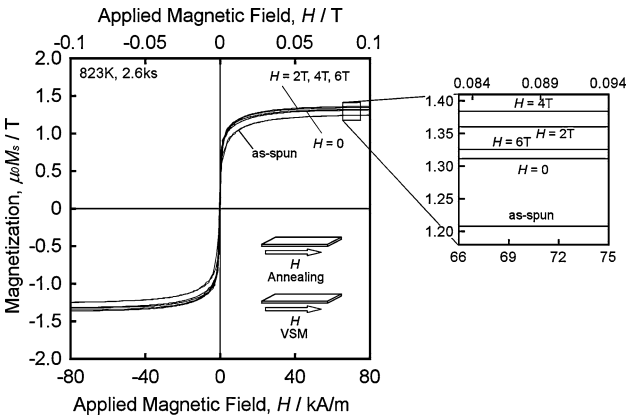

Fig. 12 Magnetization curves for $Fe_{73.5}Si_{13.5}B_9Nb_3Cu_1$ ribbons crystallized at 823 K for 2.6 ks with different magnetic-field strengths. For comparison, the curve for the as-spun amorphous ribbon is also shown

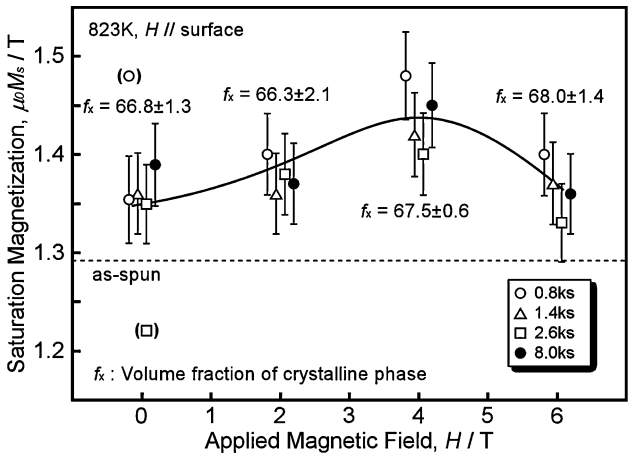

Fig. 13 Changes in saturation magnetization of $Fe_{73.5}Si_{13.5}B_9Nb_3Cu_1$ nanocrystalline ribbons as a function of magnetic-field strength applied during crystallization from amorphous precursors at 823 K for 0.8–8.0 ks. The volume fractions of the crystalline phase, f_x, are also shown

be higher than that of the amorphous alloy, and it is more enhanced by the application of a magnetic field. Figure 13 presents the saturation magnetization of the specimens measured as a function of magnetic-field strength applied during annealing. The saturation magnetization increases with increasing magnetic-field strength up to a maximum at 4 T. The change in the saturation magnetization with magnetic-field strength can be explained from the viewpoint of the boron concentration in the residual amorphous phase. Because the crystalline α-Fe(Si) phase possesses a low solid solubility for boron, boron atoms are rejected into the amorphous phase as crystallization proceeds [3, 24]. It is known that the magnetic moment of an iron atom in an Fe–B amorphous phase is a function of boron concentration [25, 26], and shows a maximum at a boron concentration of 17 at%. The atomic ratio of boron to iron is 12% in the $Fe_{73.5}Si_{13.5}B_9Nb_3Cu_1$ amorphous precursor, so that the magnetic moment of iron atoms in the residual amorphous phase increases as crystallization progresses until the ratio approaches around 17%. As mentioned in section ''Volume fraction of nanocrystallized grains in a magnetic field'', the higher the magnetic-field strength, the greater the volume fraction of crystalline phase. Therefore, it is considered that the 4 T magnetic field, where the saturation magnetization showed a maximum, yielded an optimal fraction of crystalline phase to achieve the most enhanced saturation magnetization.

Conclusions

An $Fe_{73.5}Si_{13.5}B_9Nb_3Cu_1$ amorphous precursor was crystallized by annealing at temperatures between the Curie temperature of the amorphous phase and that of the crystalline α-Fe(Si) phase in magnetic fields of up to 6 T. The texture formation and kinetics of nanocrystallization in a magnetic field were studied. The chief results obtained are as follows:

(1) The magnetic crystallization enhanced the formation of {110} texture in the α-Fe(Si) phase. Preferential nucleation, rather than preferential growth, of {110}-oriented crystals is predominantly responsible for the texture formation.
(2) Application of a magnetic field increased the nanocrystallization kinetics, particularly the nucleation rate of the ferromagnetic α-Fe(Si) grains from the paramagnetic $Fe_{73.5}Si_{13.5}B_9Nb_3Cu_1$ amorphous phase.
(3) The volume fraction of the nanocrystalline α-Fe(Si) phase increased slightly with increasing magnetic-field strength. However, thermodynamic calculations suggest that the contribution of the applied field to the Gibbs free energy is insufficient to account for the observed change in phase fraction.
(4) The saturation magnetization of the nc-$Fe_{73.5}Si_{13.5}B_9Nb_3Cu_1$ alloy increased with increasing magnetic-field strength up to a maximum at a 4 T magnetic field.

Acknowledgement The authors would like to express their hearty thanks to Profs. T. Watanabe (Tohoku University) and T. Yokobori, Jr. (Tohoku University) for their useful discussions, Dr. Iguchi (Tohoku University) for his help for X-ray measurements based on Schultz method, and to Hitachi Metals Ltd., for supplying the amorphous alloy used in this study. This work was supported by a Grant-in-Aid for Basic Research (S) (19106013) and a Grant-in-Aid for JSPS Fellows (19·3284) from the Japan Society for the Promotion of Science (JSPS). These supports are greatly appreciated.

References

1. Yoshizawa Y, Ogura S, Yamauchi K (1988) J Appl Phys 64:6044
2. Yoshizawa Y, Yamauchi K (1990) Mater Trans JIM 31:307
3. McHenry ME, Willard MA, Laughlin DE (1999) Prog Mater Sci 44:291
4. Dijkstra LJ (1954) Relation of properties to microstructure. ASM, p 209
5. Kronmüller H, Fähnle M (2003) Micromagnetism and the microstructure of ferromagnetic solids. Cambridge University Press
6. Fujii H, Tsurekawa S, Matsuzaki T, Watanabe T (2006) Phil Mag Lett 86:113
7. Häußler P, Baumann F (1980) Z Physik B 38:43
8. Wolfus Y, Yeshurun Y, Felner I, Wolny J (1987) Phil Mag B 56:963
9. Otani Y, Sun H, Coey JMD, Davis HA, Manaf A, Buckley RA (1990) J Appl Phys 67:4616
10. Wang X, Qi M, Yi S (2004) Scr Mat 51:1047
11. Willson KS, Rogers JA (1964) Tech Proc Am Electroplat Soc 51:92

12. Williams DB, Carter CB (1996) Transmission electron microscopy – spectrometry IV. Plenum Press, New York
13. van Bouwelen F, Sietsma J, de Haan CD, van den Beukel A (1992) Appl Phys Lett 61:2536
14. Allia P, Baricco M, Tiberto P, Viani F (1993) J Appl Phys 74:3137
15. Baricco M, Antonione C, Allia P, Tiberto P, Viani F (1994) Mater Sci Eng A179–180:572
16. Takahara Y (1999) J Jpn Inst Metals 63:367
17. Herzer G (1989) IEEE Trans Magn 25:3327
18. Fujii H, Matsuzaki T, Tsurekawa S (2006) In: Proceedings of 5th international symposium on electromagnetic processing of materials (EPM 2006). The Iron and Steel Institute of Japan, p 567
19. Yardley VA, Tsurekawa S, Fujii H, Matsuzaki T (2007) Mater Trans, JIM 48:2826
20. Anderson WA, Mehl RF (1945) Trans AIME 161:140
21. Okumura H, Laughlin DE, McHenry ME (2003) J Magn Magn Mater 267:347
22. Hondros ED (1970) In: Techniques of metals research, vol IV(A), Chap. 8A. Wiley, New York
23. Hondros ED, Stuart LEH (1968) Phil Mag 17:711
24. Wu YQ, Bitoh T, Hono K, Makino A, Inoue A (2001) Acta Mater 49:4069
25. Cowlam N, Carr GE (1985) J Phys F: Met Phys 15:1109
26. Hafner J, Tegze M, Becker Ch (1994) Phys Rev B 49:285